Supporting Information

Double Amidino-Mediated Multiple Hydrogen-Bonded Dion-Jacobson Perovskites Enable Oriented Crystallization for Efficient Inverted $FAPbI_3$ Solar Cells and Modules (642 cm^2)

Zhiyuan Xu,[1,#] Yuqin Zhou,[1,#] Cheng Gong,[1,#] Ke Wang,[1] Zhihao Guo,[1] Zhijun Li,[1] Omar F. Mohammed,[2,*] and Zhigang Zang[1,*]

[1]Key Laboratory of Optoelectronic Technology & Systems (Ministry of Education), Chongqing University, Chongqing 400044, China

[2]Center for Renewable Energy and Storage Technologies (CREST) Division of Physical Sciences and Engineering, King Abdullah University of Science and Technology (KAUST), Thuwal 23955-6900, Kingdom of Saudi Arabia

[#]The authors contributed equally to this work.

*Correspondence Authors: omar.abdelsaboor@kaust.edu.sa (Omar F. Mohammed); zangzg@cqu.edu.cn (Zhigang Zang)

Experimental Section

Materials

Cesium iodide (CsI), formamidinium iodide (FAI), lead iodide (PbI_2), and PCBM were purchased from Advanced Election Technology Co., Ltd. The nickel nitrate hexahydrate ($Ni(NO_3)_2 \cdot 6H_2O$), sodium hydroxide (NaOH), dimethylformamide (DMF), dimethyl sulfoxide (DMSO), isopropanol (IPA), Chlorobenzene (CB), and Al_2O_3 dispersions were obtained from Sigma Aldrich. [4-(3, 6-dimethyl-9H-carbazol-9-yl)butyl]phosphonic acid (MeO-2PACz) was obtained from TCI America. Bathocuproine (BCP) was purchased from Xi'an Yuri Solar Co., Ltd. Benzamidine dihydrochloride (PhFACl) and benzdiamidine dihydrochloride ($PhDFACl_2$) were obtained from Macklin. All the chemicals and reagents were used directly without further purification.

Device fabrication

The ITO-coated glass substrates were laser-etched, followed by ultrasonic cleaning of the etched ITO glass for 15 min using a detergent, deionized water (twice), ethanol (twice), and isopropanol (twice) in sequential order. The ITO-coated glass substrates were subjected to a 20-minute treatment of ultraviolet-ozone (UVO). Subsequently, a NiO_x NPs aqueous ink with a concentration of 30 mg/mL was prepared by dispersing the as-prepared NiO_x NPs in deionized water. This ink was then spin-coated onto the ITO glass at a speed of 5000 rpm for 30 s. The NiO_x films (~20 nm) were annealed at 100 ℃ for 10 min, followed by immediate transfer into a nitrogen-filled glove box. MeO-2PACz solution (0.5 mg mL^{-1} in IPA) was spin-coated on the NiO_x-covered substrates at 3000 rpm for 30 s, followed by thermal annealing at 100 ℃ for 10 min. Subsequently, the MeO-2PACz films (~4 nm) were spin-coated with an Al_2O_3 dispersion solution (0.4 wt% in IPA) at 5000 rpm for 30 s. The control $FA_{0.95}Cs_{0.05}PbI_3$ precursor solution was prepared by dissolving 228.4 mg of FAI, 18.2 mg of CsI, 645.4 mg of PbI_2 in a mixed solvent solution (v/v, DMF : DMSO = 4 : 1) with a concentration of 1.4 mol/L. For the modified 2D/3D perovskite precursor solution, PhFACl (1.0 mg) or $PhDFACl_2$ (1.0 mg) was added to $FA_{0.95}Cs_{0.05}PbI_3$ perovskite precursor solution for

modification. The perovskite precursor solution was then spin-coated onto a glass/ITO/NiO_x/MeO-2PACz/Al_2O_3 substrate at speeds of 2000 rpm for 10 s followed by an additional spin at 4000 rpm for 40 s. During the second spin coating step, 150 μL of CB was deposited onto the perovskite film 5 seconds before the program ended. The resulting wet perovskite films were annealed at 100 ℃ for 30 min. Subsequently, a solution of $PC_{61}BM$ in CB with a concentration of 23 mg/mL was spin-coated onto the perovskite films (~600 nm) at a speed of 2500 rpm for 40 s. Afterwards, a solution of BCP in IPA with a concentration of 0.5 mg/mL was spin-coated on top of the $PC_{61}BM$ film (~30 nm) at a speed of 5000 rpm for 30 s to obtain BCP layer (~5 nm). Finally, a thermal evaporation process under vacuum conditions (2×10^5 Pa) was employed to deposit a Ag electrode with thickness around 100 nm.

For the modules, first, use Physical Vapor Deposition (PVD) technology to prepare NiO_x with a thickness of approximately 18 nm on the FTO substrate. The $FA_{0.83}Cs_{0.17}PbI_3$ perovskite film is prepared by dissolving 0.2086 g of $PbCl_2$, 1.325 g of CsI, 15.213 g of PbI_2, 4.282 g of FAI, and 36 mg of $PhDFACl_2$ in a 30 ml mixed solvent solution (v/v, DMF: NMP: ACN = 6: 1: 3) with a concentration of 1.1 mol/L. The perovskite precursor solution is then slot-die coated onto a glass/ FTO/NiO_x substrate with a slot-die gap of 100 μm above the substrate at a speed of 5 mm/s. Then, the resulting wet perovskite films are quickly transferred into a vacuum chamber, which is pumped to 10 Pa and maintained for 40 s. The resulting perovskite films are then annealed at 150 ℃ for 15 min in the air (RH = 20%). Subsequently, the PCBM solution (23 mg/mL) is then slot-die coated onto the perovskite film with a slot-die gap of 100 μm at a speed of 4 mm/s. 20 nm of ALD-SnO_2 is deposited on the PCBM surface. Finally, the ITO/Cu/ITO sandwich electrodes are pre pared on the ALD-SnO_2 surface using PVD technology, with thicknesses of 20 nm/15 nm/20 nm, respectively.

Characterizations

The *J–V* characteristics of inverted PSCs were measured under 1 sun equivalent illumination in ambient conditions using a Keithley source meter (2400) and the solar simulator, which equipped a 450 W Xenon lamp (Newport 2612 A, Oriel Sol3A). The

light intensity was controlled at AM 1.5G (100 mW cm^{-2}) by a standard silicon solar cell. The exposure area of metal mask in *J–V* measurements was 0.1 cm^2. The external quantum efficiency (EQE) was collected by using a QE-R Solar Cell Spectral Response Measurement System (Enli Technology Co., Ltd., Taiwan). The liquid-state ^1H NMR measurements were conducted in d_6-DMSO using a Bruker 400 MHz measurement spectrometer. The FTIR spectra were collected by the Nicolet iS50 system of Thermo Fisher Scientific. The XPS spectroscopy was obtained by using the Thermo Scientific ESCALAB 250Xi at Shiyanjia lab (www.Shiyanjia.com). XPS was calibrated using binding energy of C1s (284.80 eV) as the energy standard. In the measured C element spectra, the C-C binding energy positions of control, PhFA-based and PhDFA-based films are 283.46 eV, 284.13 eV, and 284.23 eV, which are smaller than 284.80 eV. Therefore, all of the examined spectra are selected, and 1.34 eV, 0.67 eV, and 0.57 eV are added for control, PhFA-based, and PhDFA-based films to complete the XPS results calibration. The UPS measurements were conducted by PHI 5000 Versaprobe at Shiyanjia lab (www.Shiyanjia.com). The GIWAXS measurements were conducted at Beijing Synchrotron Radiation Facility (BSRF), 1W1A station, using X-ray with a wavelength of 1.54792 Å, and the incident angle was 0.2°. The surface and cross-sectional SEM images were scanned by Zeiss Merlin Compact of Germany. The AFM measurements were conducted by Bruker Dimension Icon (Germany). Contact angle measurement was taken on a JC2000D1 (Shanghai Zhongchen) contact angle instrument. The XRD patterns were collected by Rigaku Ultima IV (Japan). The GIXRD patterns were collected by PANalytical Empyrean (Netherlands). The UV-vis absorption spectra were obtained via the Shimadzu UV-3600 spectrometer. Steady-state PL and TRPL were performed by a fluorescence spectrophotometer (FLS1000, Edinburgh Instruments Ltd.) PL mapping was collected via Laser Ramon Instrument (LabRAM HR Evolution). TPC and TPV measurements were conducted using a system excited by a 532 nm (1000 Hz, 6 ns) pulsed laser. The Mott–Schottky and EIS plots were obtained by an electrochemical workstation (CHI 660). The dark J-V characteristic of devices was obtained via the Keithley source meter.

SCLC measurements. Necessary preparations such as calibrating the test equipment and assuring the consistency of the single electron or hole device fabrication procedure were conducted. Setting the frequency and time of data collection, as well as other SCLC testing parameters. The I-V characteristic curve is obtained by applying voltage (0-3V) to the PSCs and recording the related current value. For data processing, the current and voltage data obtained from the test are taken logarithmically and plotted into a curve. In the log coordinate, there are three segments: n=1, n>3, and n=2. Note that n represents the slope of the apparent fit of the I-V curve under double logarithm. Following that, determining the horizontal coordinate that corresponds to the intersection of the two tangents on the log(I)-log(V) curve for n=1 and n>3, which is the trap-filled limit voltage (V_{TFL}). Finally, the defect state density is calculated according to the SCLC model formula.

UPS measurements. The sample surface was ensured to be flat and free of contamination before testing, and then cleaned with an ion source. To ensure data reliability, avoid contacting the atmosphere from sample preparation to the test chamber. The light source during the test was He-Iα rays with a photon energy of 21.2 eV. The beam diameter is 5.0 um. Energy calibration is the initial step in data processing to guarantee the veracity of the data. Due to the data being biassed by -5 eV, an addition of 5 eV is required for calibration. The calibrated data were plotted in segments (0-2 eV and 15-18 eV). Drawing a tangent to the high binding energy side (secondary electron cutoff side) and obtaining the intersection value with the tangent line on the same side (parallel to the X-axis). After that, the work function is obtained by subtracting the intersection value from 21.2. Similarly, a tangent is drawn on the low binding energy side (Fermi edge), and the intersection with the tangent on the same side (parallel to the X-axis) represents the valence band top.

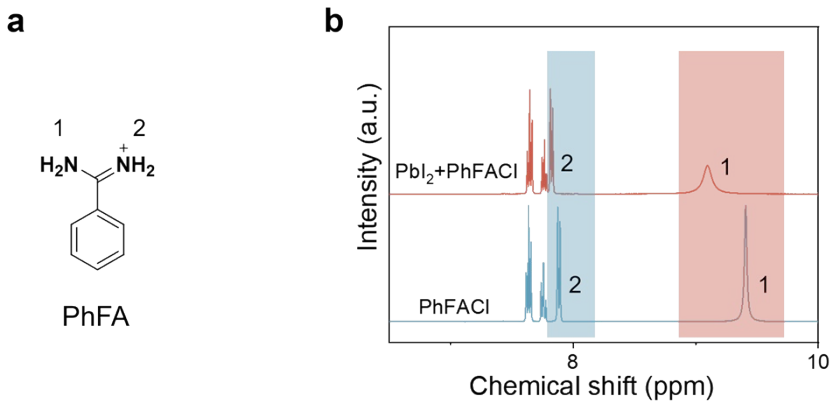

Fig. S1. ^{1}H NMR spectra of PhFACl, and PbI_2 + PhFACl.

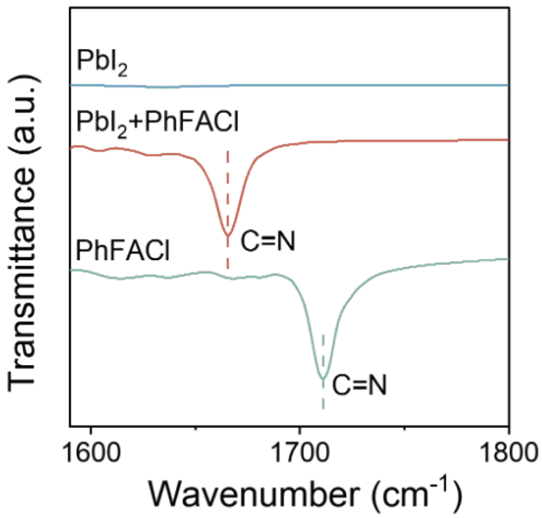

Fig. S2. Spectrums of FTIR for PhFACl, PbI_2, and PbI_2 combined with PhFACl for C═N stretching peaks.

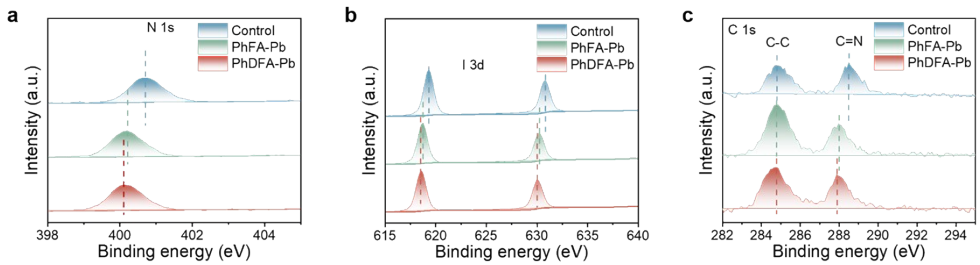

Fig. S3. XPS spectra of corresponding perovskite films.

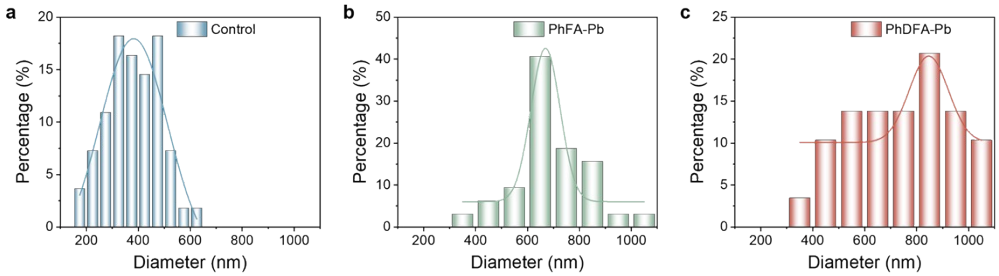

Fig. S4. The corresponding statistical graphic of average grain size for corresponding perovskite films.

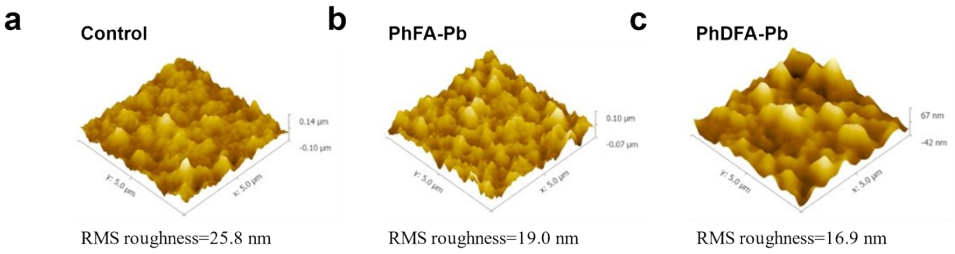

Fig. S5. AFM images of corresponding perovskite films.

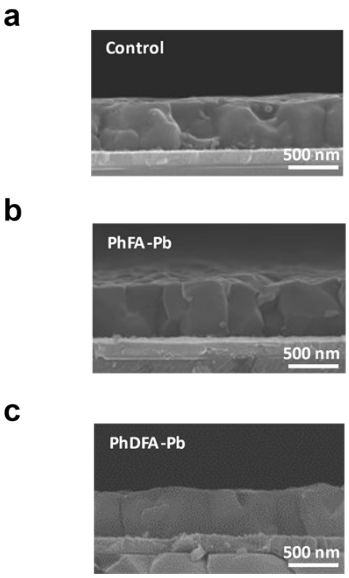

Fig. S6. Cross-sectional SEM images for corresponding perovskite films.

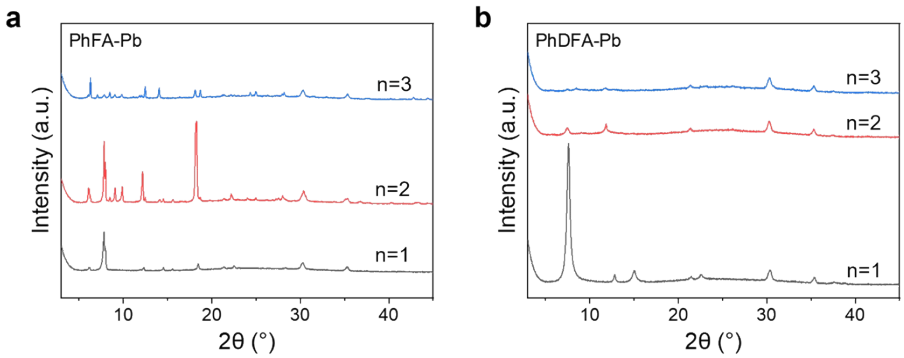

Fig. S7. XRD patterns of the PhFA-Pb and PhDFA-Pb films with different n values (n = 1-3).

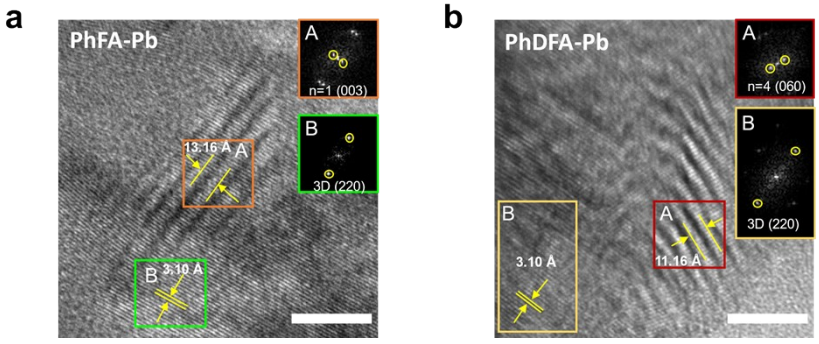

Fig. S8. HRTEM of the PhFA-based 2D/3D and PhDFA-based 2D/3D perovskite film and Fast Fourier transforms (FFT) of the of selected area diffraction.

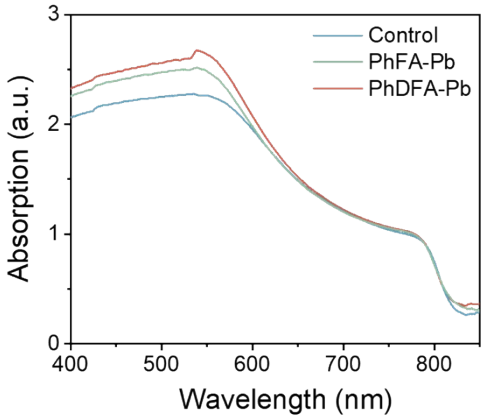

Fig. S9. UV–vis absorption spectra for corresponding perovskite films.

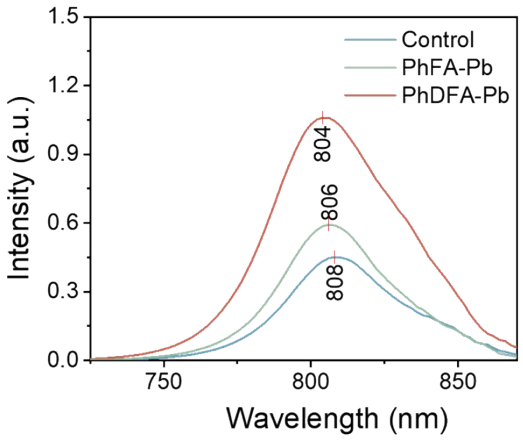

Fig. S10. PL spectra of corresponding perovskite films.

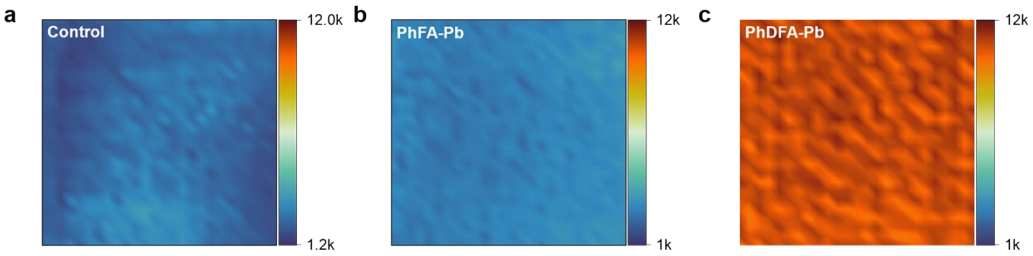

Fig. S11. PL mapping of corresponding perovskite films.

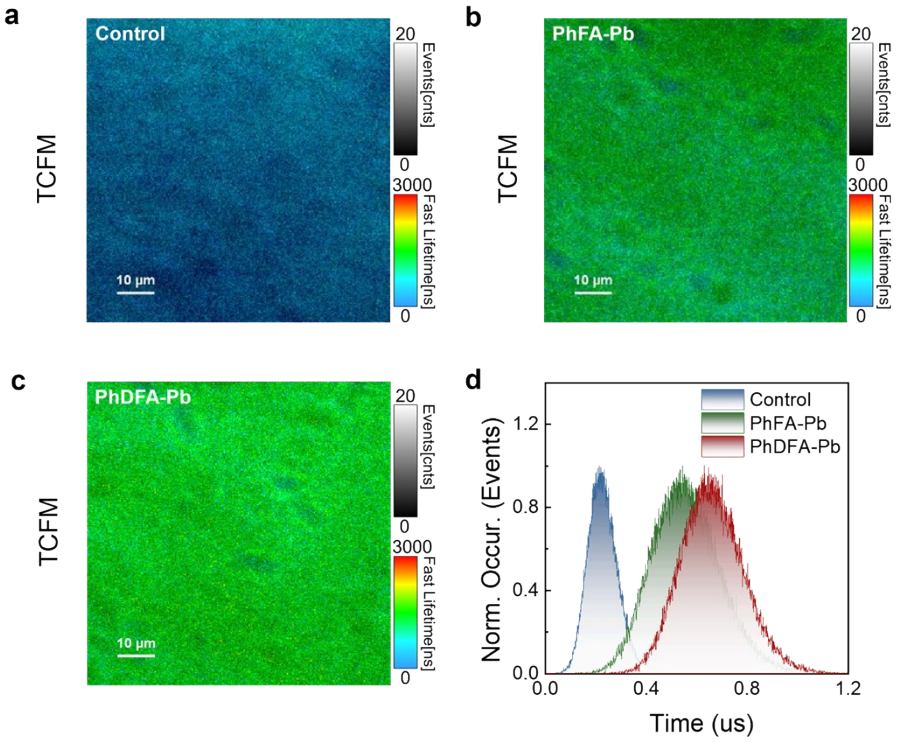

Fig. S12. The TCFM images of corresponding films.

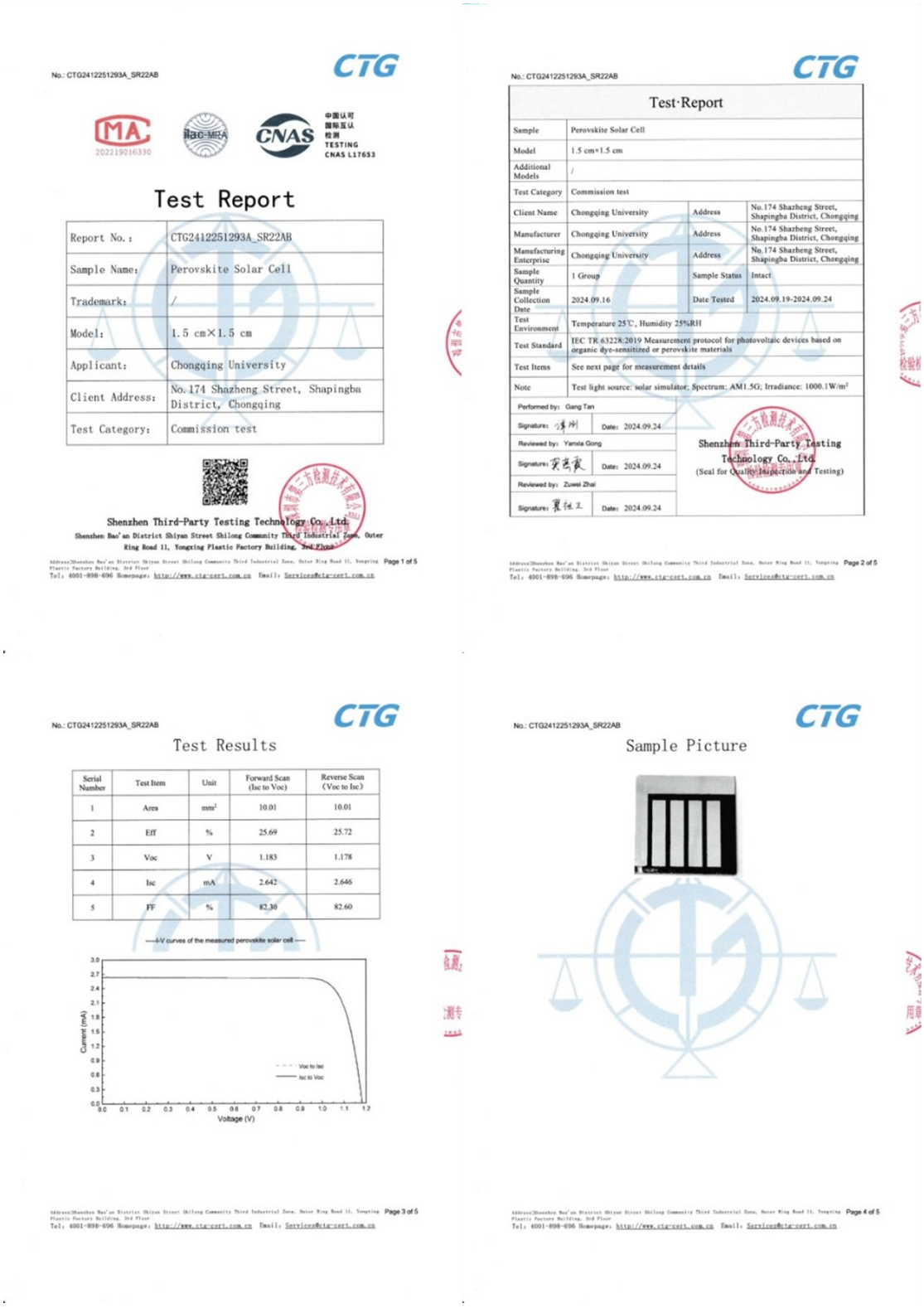

Fig. S13. Independent certification of one of the best-performing PhDFA-based 2D/3D devices.

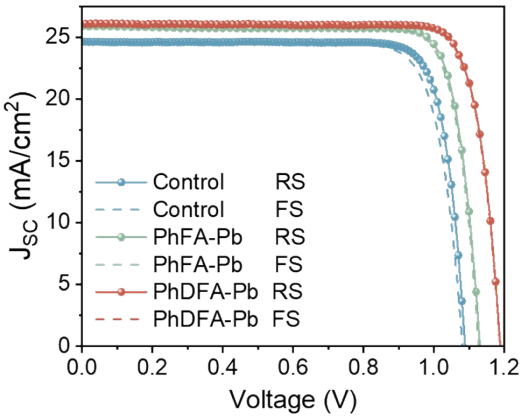

Fig. S14. *J–V* curves for corresponding device under forward and reverse scan directions.

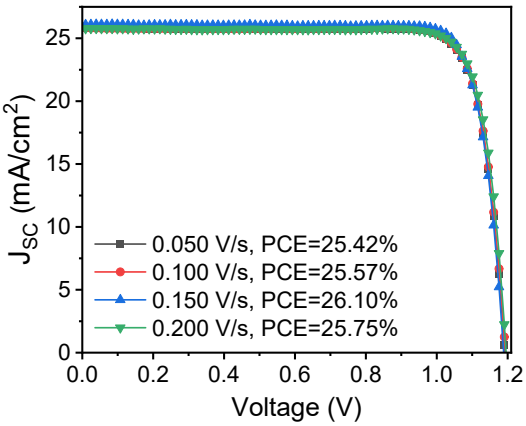

Fig. S15. *J–V* curves of the 2D/3D hybrid perovskite device measured under different scan rates.

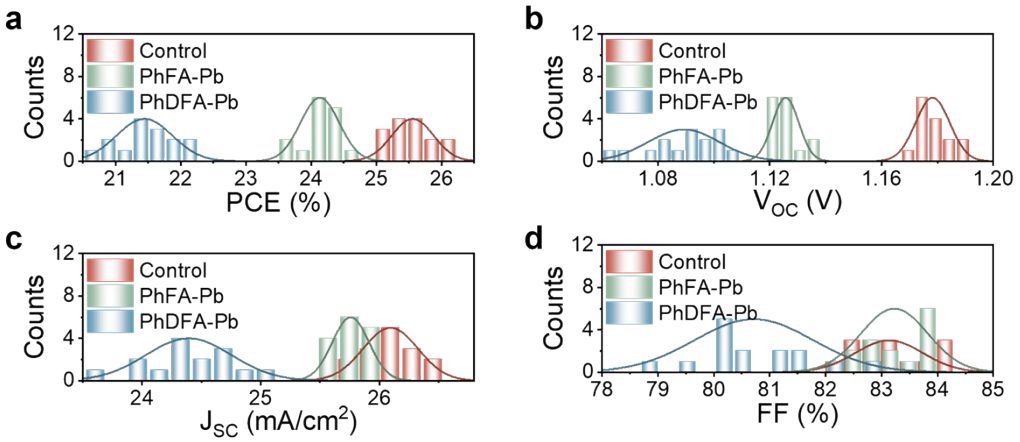

Fig. S16. Statistical box diagram of PV parameters for corresponding devices. Each set of data used for the statistical graph has 15 individual devices.

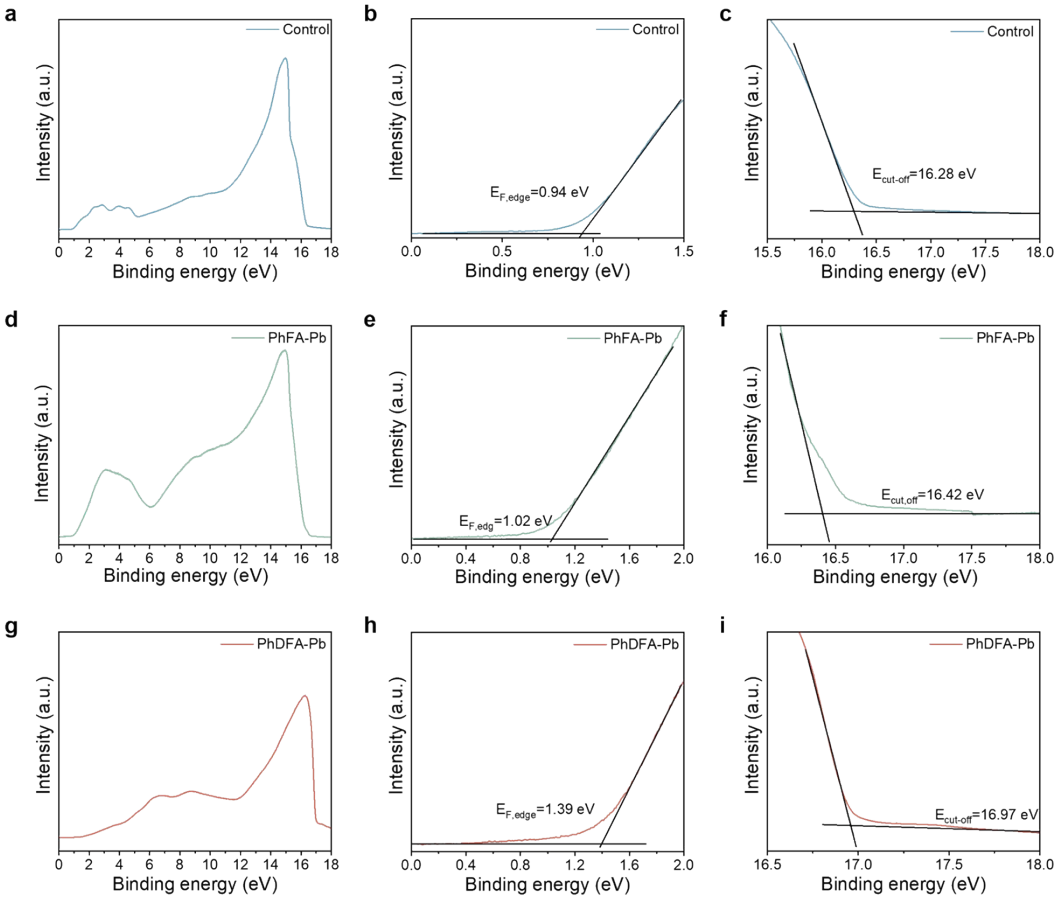

Fig. S17. UPS spectra of full-scale region, cut-off region, and onset region for corresponding films.

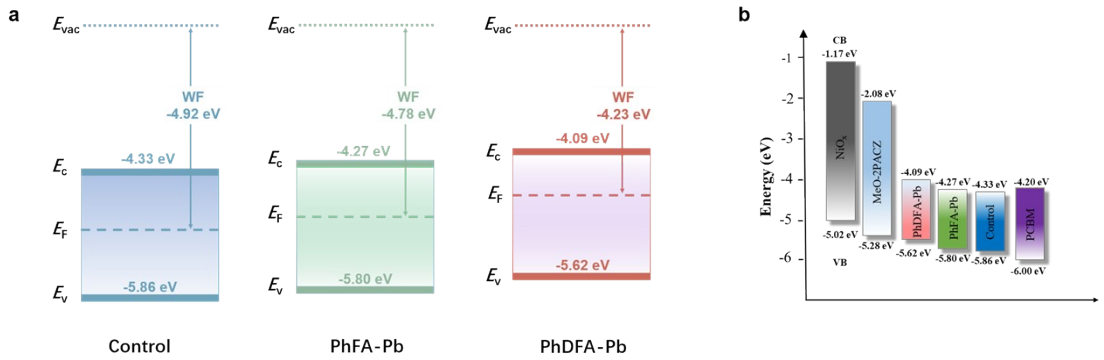

Fig. S18. Band alignment diagram of perovskite film with PhFACl and $PhDFACl_2$ before and after modification.

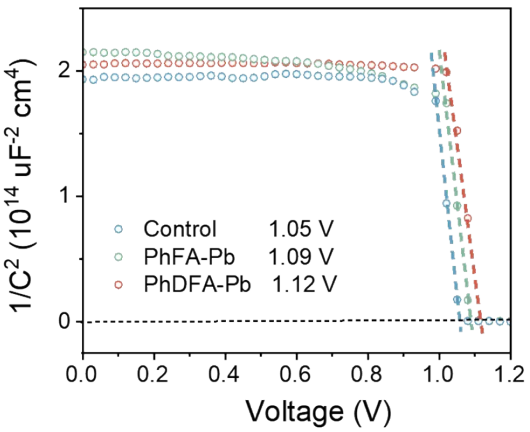

Fig. S19. Mott–Schottky plots of corresponding devices.

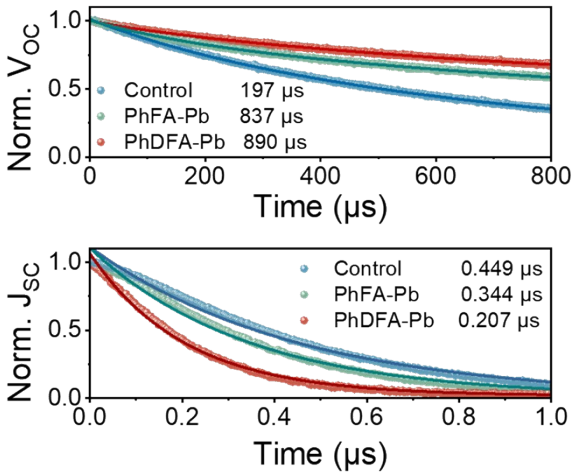

Fig. S20. TPV and TPC curves for corresponding devices.

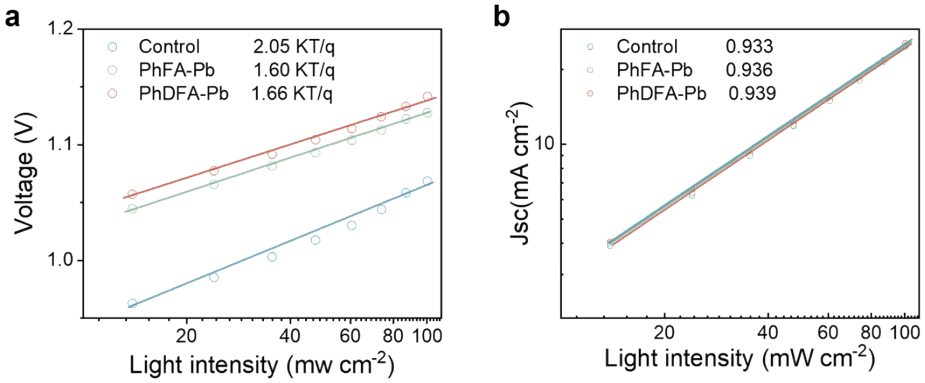

Fig. S21. V_{OC} and J_{SC} versus light intensity for the corresponding devices.

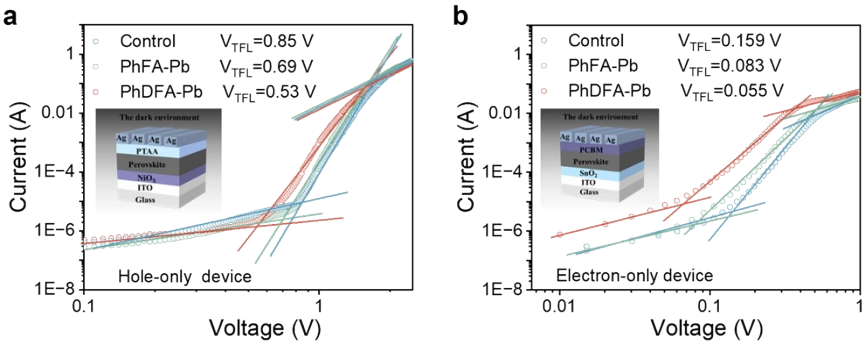

Fig. S22. The I−V curves of the hole-only devices and the electron-only devices.

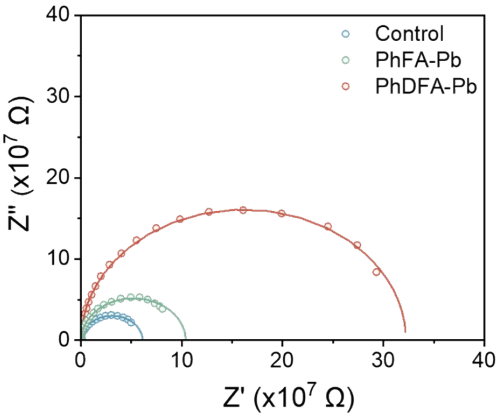

Fig. S23. Electrochemical impedance spectroscopy (EIS) measurements for corresponding PSCs.

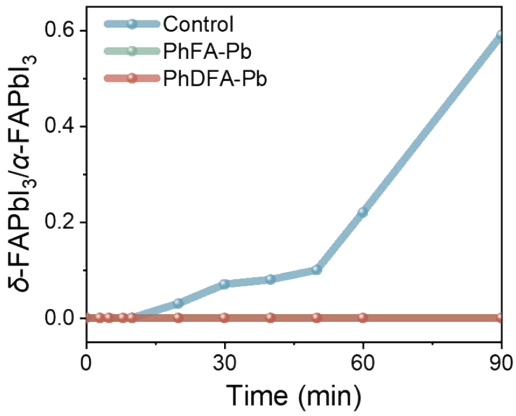

Fig. S24. The intensity ratio of δ-$FAPbI_3$ and α-$FAPbI_3$ XRD peaks in corresponding perovskite films.

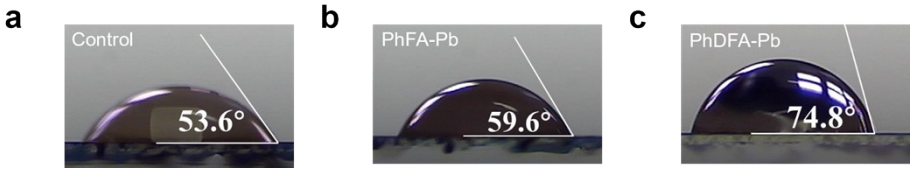

Fig. S25. Contact angle of corresponding perovskite films.

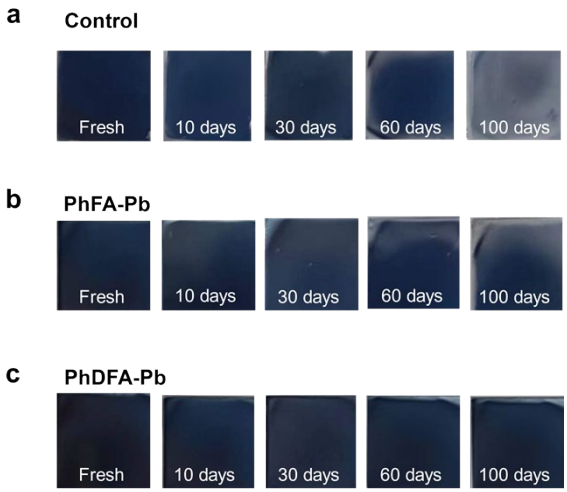

Fig. S26. The photographs of corresponding perovskite films after aging 100 days.

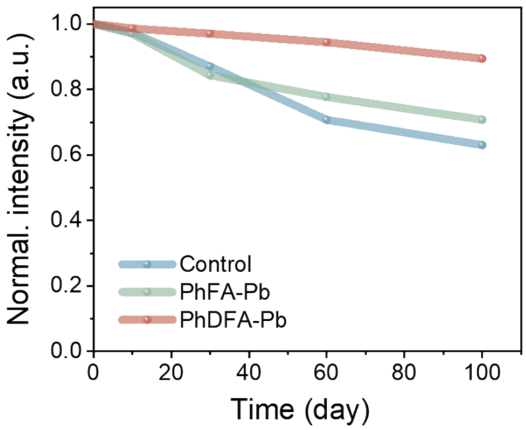

Fig. S27. The intensity of 500 nm in UV-vis spectra for corresponding films in the aging procedure.

Table S1. The fitted results of TRPL curves for perovskite films. The average lifetime was calculated using the equation $\tau_{ave} = \frac{\sum A_i \tau_i^2}{\sum A_i \tau_i}$.

Samples	τ_1 (ns)	A_1	τ_2 (ns)	A_2	τ_{avg} (ns)
Control	290.59	62.05	955.62	37.95	734.75
PhFA-Pb	405.28	48.6	2024.06	51.4	1766.08
PhDFA-Pb	900.68	54.57	3528.23	45.42	2911.59

Table S2. Photovoltaic parameters of corresponding devices.

Device		V_{OC} (V)	J_{SC} (mA cm^{-2})	FF	PCE (%)
Control	Average	1.09±0.010	24.36±0.31	0.808±0.006	21.40±0.37
	Champion	1.09	24.63	0.830	22.27
PhFA-Pb	Average	1.12±0.002	25.60±0.017	0.837±0.004	24.10±0.17
	Champion	1.13	25.88	0.837	24.48
PhDFA-Pb	Average	1.18±0.008	26.09±0.18	0.839±0.005	25.56±0.25
	Champion	1.19	26.08	0.841	26.10

Table S3. Photovoltaic parameters of corresponding devices under different scanning directions.

Device		V_{OC} (V)	J_{SC} (mA cm^{-2})	FF	PCE (%)
Control	Reverse	1.09	24.63	0.830	22.27
	Forward	1.09	24.61	0.802	21.51
PhFA-Pb	Reverse	1.13	25.88	0.837	24.48
	Forward	1.13	25.69	0.838	24.33
PhDFA-Pb	Reverse	1.19	26.08	0.841	26.10
	Forward	1.19	26.08	0.840	26.07

Table S4. The photovoltaic performance of inverted DJ 2D/3D PSCs in our work was compared to previous literatures that reported both regular and inverted DJ 2D/3D PSCs.

Device structure	V_{OC} (V)	J_{SC} (mA cm^{-2})	FF (%)	PCE (%)	Year	Ref.
Regular	1.13	24.8	80.5	22.6	2021	1
Regular	1.15	25.88	76.66	22.68	2021	2
Inverted	1.09	23.61	78.53	20.21	2022	3
Regular	1.15	25.6	79.9	23.6	2022	4
Regular	1.14	24.8	84.7	23.95	2022	5
Regular	1.158	25.25	84.3	24.7	2022	6
Inverted	1.15	24.8	82.8	23.62	2023	7
Inverted	1.19	23.47	84.5	23.60	2023	8
Regular	1.18	25.70	81.81	24.9	2023	9
Regular	1.181	26.04	82.21	25.3	2023	10
Inverted	1.181	25.71	83.2	25.26	2023	11
Regular	1.09	24.1	77.60	20.40	2024	12
Inverted	**1.19**	**26.08**	**84.1**	**26.10**	**2024**	**This work**

Table S5. The calculated trap density and mobility for corresponding devices.

Device	N_t^e ($\times 10^{15}$) [cm^{-3}]	N_t^h ($\times 10^{15}$) [cm^{-3}]	μ_e ($\times 10^{-3}$) [$cm^3\ V^{-1}\ s^{-1}$]	μ_h ($\times 10^{-3}$) [$cm^3\ V^{-1}\ s^{-1}$]
Control	0.87	4.65	1.26	2.23
PhFA-Pb	0.45	3.76	3.03	3.99
PhDFA-Pb	0.30	2.91	5.23	5.7

References

1 T. Niu, Y.-M. Xie, Q. Xue, S. Xun, Q. Yao, F. Zhen, W. Yan, H. Li, J.-L. Brédas, H.-L. Yip and Y. Cao, *Adv. Energy Mater.* 2022, 12, 2102973.

2 Y. Zhong, G. Liu, Y. Su, W. Sheng, L. Gong, J. Zhang, L. Tan and Y. Chen, *Angew. Chem. Int. Ed.* 2022, 61, e202114588.

3 W. Zhou, L. Jia, M. Chen, X. Li, Z. Su, Y. Shang, X. Jiang, X. Gao, T. Chen, M. Wang, Z. Zhu, Y. Lu and S. Yang, *Adv. Funct. Mater.* 2022, 32, 2201374.

4 X. Wei, M. Xiao, B. Wang, C. Wang, Y. Li, J. Dou, Z. Cui, J. Dou, H. Wang, S. Ma, C. Zhu, G. Yuan, N. Yang, T. Song, H. Zhou, H. Chen, Y. Bai and Q. Chen, *Angew. Chem. Int. Ed.* 2022, 61, e202204314.

5 C. Luo, G. Zheng, F. Gao, X. Wang, Y. Zhao, X. Gao and Q. Zhao, *Joule* 2022, 6, 240-257.

6 F. Zhang, S.Y. Park, C. Yao, H. Lu, S.P. Dunfield, C. Xiao, S. Uličná, X. Zhao, L. Du Hill, X. Chen, X. Wang, L.E. Mundt, K.H. Stone, L.T. Schelhas, G. Teeter, S. Parkin, E.L. Ratcliff, Y.-L. Loo, J.J. Berry, M.C. Beard, Y. Yan, B.W. Larson and K. Zhu, *Science* 2022, 375, 71-76.

7 Y. Zheng, X. Wu, R. Zhuang, C. Tian, A. Sun, C. Tang, Y. Liu, Y. Hua and C.-C. Chen, *Adv. Funct. Mater.* 2023, 33, 2300576.

8 S. Ramakrishnan, D. Song, Y. Xu, X. Zhang, G. Aksoy, M. Cotlet, M. Li, Y. Zhang and Q. Yu, *Adv. Energy Mater.* 2023, 13, 2302240.

9 T. Yang, C. Ma, W. Cai, S. Wang, Y. Wu, J. Feng, N. Wu, H. Li, W. Huang, Z. Ding, L. Gao, S. Liu and K. Zhao, *Joule* 2023, 7, 574-586.

10 T. Yang, L. Gao, J. Lu, C. Ma, Y. Du, P. Wang, Z. Ding, S. Wang, P. Xu, D. Liu, H. Li, X. Chang, J. Fang, W. Tian, Y. Yang, S. Liu and K. Zhao, *Nat. Commun.* 2023, 14, 839.

11 C. Gong, X. Chen, J. Zeng, H. Wang, H. Li, Q. Qian, C. Zhang, Q. Zhuang, X. Yu, S. Gong, H. Yang, B. Xu, J. Chen and Z. Zang, *Adv. Mater.* 2024, 36, 2307422.

12 J. Tang, Y. Lin, H. Yan, J. Lin, H. Rao, Z. Pan and X. Zhong, *Angew. Chem. Int. Ed.* 2024, 63, e202406167.